Project of Strategic Interest NEXTDATA

Deliverable D1.2.4
Report describing the activities, data transfer to archives and to the General Portal

WP Coordinator: Angela Marinoni
CNR-ISAC

P. Cristofanelli, A. Marinoni, R. Duchi, D, Putero, T. Landi, F. Calzolari and P. Bonasoni
CNR-ISAC, Bologna

E. Vuillermoz, R. Toffolon, M. Alborghetti, G. Verza
EV-K2-CNR, Bergamo

J. Arduini, M. Maione
Urbino University, Urbino

R. Balestrini
CNR-IRSA, Brugherio

Italian Institutions are managing two Global Stations belonging to the GAW/WMO programme: the Italian Climate Observatory "O. Vittori" at Monte Cimone (2165 m. a.s.l., northern Apennines) and the Nepal Climate Observatory – Pyramid (5079 m. a.s.l., Nepal). Thanks to their location at high altitudes, the measurements performed at these Global Stations are considered well representative of wide geographical areas, which allows an effective characterization of atmospheric variability over large regions and long time frames for two hot-spot regions (the Mediterranean basin and the Himalayas) particularly affected by anthropogenic pressures and climate change. Here we provide information on the activities, data transfer to archives and to the General Portal during the second year of the NextData Project. The results of these activities were possible thanks to the collaboration of different Institutions: CNR-ISAC, EV-K2-CNR, University of Urbino, ENEA-UTMEA, CNR-IRSA.
The observations and study activities have been continued at the GAW/WMO global station Monte Cimone (GAW ID: CMN) and Nepal Climate Observatory – Pyramid (GAW ID: PYR). Within this framework, activities were carried out concerning instrument calibrations and data validations for trace gases (greenhouse and reactive), atmospheric aerosol (chemistry and physics), precipitation (rain and snow chemistry), meteorological parameters and solar radiation fluxes (short-wave and long-wave) observations, according to the guidelines of the GAW/WMO and BSRN (Baseline Surface Radiation Network) programme.
The temporal availability, for the year 2013, of the measurements in the framework of GAW/WMO, is reported in the Annex 1, for the two Global Stations "O. Vittori" – Monte Cimone and Nepal Climate Observatory – Pyramid.
During the reference period, data of atmospheric composition, meteorology and precipitation chemistry were submitted to the GAW/WMO data-bases
(http://ds.data.jma.go.jp/gmd/wdcgg/, http://ebas.nilu.no/Default.aspx, http://wdpc.org). Data were also shared with the NextData General Portal by submission to the GeoNetwork system (WP2.1).
Thanks to an agreement with RSE SpA (Ricerca sul Sistema Elettrico SpA) and CNR-ISAC (signed in December 2013), the greenhouse gas data (CO_2, CH_4, O_3) were shared with NextData; the historical data sets were submitted to the GeoNetwork database and a system for delivery of data in near-real-time (NRT) was implemented by RSE SpA to provide every hour greenhouse gas mixing ratios. By means of CNR-ISAC, which will be in charge of the data formatting and delivery to ECMWF (European Center for Medium range Weather Forecast), these NRT data will be made available to the MACC-2 Project (see deliverable D1.1.1).
CNR-ISAC supported the University of La Paz in the execution of surface ozone measurements at the GAW/WMO atmospheric observatory at Chacaltaya (Bolivia). In particular, during the reference period, CNR-ISAC provided technical and scientific instructions on how to solve instrumental issues and to perform data validation; to this aim, semi-automatic procedures for the screening and flagging of data were shared.

Activities at the Nepal Climate Observatory – Pyramid (NCO-P)

During year 2013, CNR-ISAC, EV-K2-CNR, ENEA-UTMEA and CNR-IRSA continuously supported (by remote) the local staff for the execution of the measurement programmes running at NCO-P.

During March – April 2013, a maintenance campaign was undertaken at NCO-P for the checking and calibrating of the experimental set-up. Technicians and researchers from URT Ev-K2-CNR, CNR-ISAC, LGGE-CNRS and the Pyramid personnel participated in this campaign. In particular, during this experimental campaign, the system for the measurement of the

aerosol size distribution of particles with diameters from 10 nm to 800 nm were dismounted and transported to the CNRS-LGGE laboratories (France) for the execution of upgrade activity to fulfill the GAW/ACTRIS standard quality. To avoid a complete data gap during the upgrade activities, a condensation particle counter (CPC, TSI 3010) was installed at the NCO-P; it provides the integrated counting of aerosol particles with diameters from 10 nm to 3µm.

CMR-ISAC Bologna coordinated the activities to re-start the PM1-PM10 measurements by the b-absorption system which were stopped in Summer 2012 due to an internal water flood during the Summer monsoon. Moreover, the ozone analyser Thermo 49c was replaced by a newer Thermo 49i. With the aim of keeping the measurements well tracked to the GAW-WMO reference scale, the analyses was calibrated at the World Calibration Center hosted at EMPA (Switzerland) before shipping to Nepal. In collaboration with ENEA-UTMEA, a new pirgeometer CMP23 was installed at the station and the pyranometer CMP21 was maintained. To this purpose, the radiometry acquisition system was upgraded during the field campaign.
In 2013 a new collaboration between CNR-ISAC and Stockholm University was established, with the goal of measuring the ratio of Carbon isotopes in the aerosol particles at NCOP, useful for evaluating the fractionation of BC from different sources (e.g. . fossil vs biomass) at NCO-P (see more on Deliverable D1.2.5). A special protocol for aerosol sampling, based on the use of a high volume PM10 sampler, was developed together with Stockholm University and the Nepali local staff was trained for this new activity during calibration campaign in Spring 2013.
Moreover, a feasibility study to execute an experimental campaign for the investigation of the new particle formation events during the post-monsoon season was carried out in collaboration with the Helsinki University and the "Paul Sherrer" Institute. To this aim, a preparation meeting was organized in Lecco in September 2013. The main purpose was to investigate which gas compounds are involved in the new particle formation processes and how they can influence the growth of the particles.

Research activity: wet precipitation period

In collaboration with CNR-IRSA, within the GAW/WMO programme, the chemistry and the isotopic composition (stable isotopes of oxygen and deuterium) of wet deposition were investigated at the Pyramid International Laboratory, during the 2012 monsoon season. The snow precipitation which occurred in Winter and Spring 2013 were analysed as well. The data were elaborated also integrating the results obtained by the earlier monitoring, performed during the 2007- 2008 period. The achieved results are summarized below:

1- In the analysed rain samples, the major cations were NH_4^+ and Ca_2^+. HCO_3^- represented about 70% of the anions, followed by $NO_3^- > SO_4^{2-} > Cl^-$. Data treatment suggests that Na^+, Cl^- and K^+ were related to long range transport of marine aerosols; Ca_2^+, Mg_2^+ and HCO_3^- were related to the contribution of rock and soil dust; NO_3^- and SO_4^{2-} were related to anthropogenic sources; NH_4^+ were related to the scavenging of gaseous NH_3.
2- The temporal variations of NO_3^- and SO_4^{2-} exhibited maximum concentrations at the beginning and ending phases of monsoon (see Fig. 4). The NH_4^+ enrichment in July was probably due to the local transport from low-lying valley dominated by cultivated land and vegetated soil.

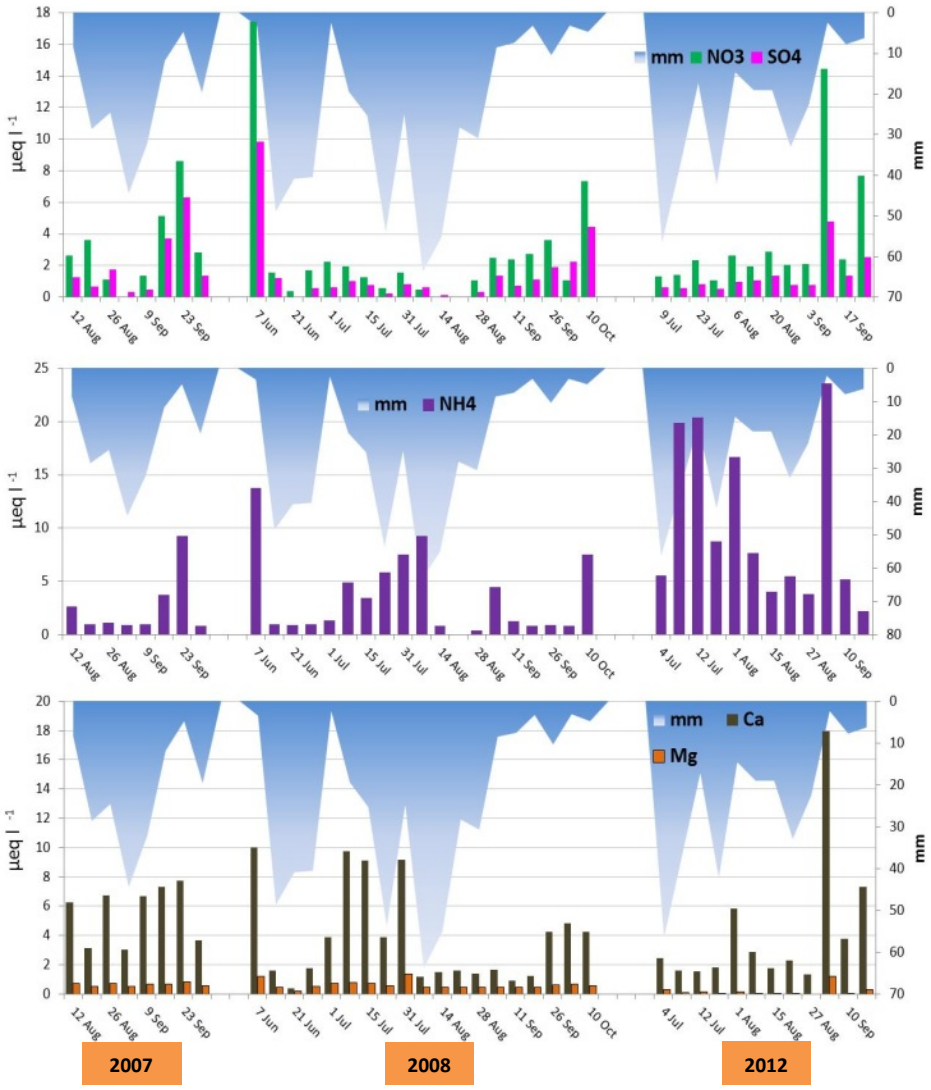

Fig. 1. Temporal trends of the main ionic species in weekly precipitation samples collected during 2007, 2008 and 2012 (CNR-IRSA).

3- Also the isotopic composition is strongly influenced by the amount of precipitation, with depleted values characterizing the central monsoon period.

4- Wet deposition chemistry results indicated that, during Summer, the presence of anthropogenic species, especially NO_3^- and SO_4^{2-} (tracers of fossil fuel combustion), was really scarce, thus indicating the occurrence of background atmosphere conditions.

5- The low nitrogen concentrations associated with very modest amounts of precipitation have produced nitrogen loads considerably lower (0.30-0.49 kg ha^{-1} yr^{-1}) than those measured in high-altitude environments in Europe and North America. Higher N loads were reported for other different ecosystems in the most remote regions of the world, as the Northern Africa dry savannah and the Central Amazonia tropical rain forest.

6- For specific chemical species (NO_3^-, NH_4^+, SO_4^{2-}), the analysis of snow samples reveals some concentrations considerably higher than those measured for rain samples: these findings support the hypothesis that during non-monsoon periods the region is affected by the presence of air masses relatively contaminated and, in addition, indicate that the dry deposition deposited on the snowpack during winter could contribute to the total deposition fluxes of nitrogen species and other compounds.

Research activity: Influence of open vegetation fires on black carbon and ozone variability in the southern Himalayas

NCO-P observations were analysed to assess the influence of open vegetation fires on *Short-lived climate forcers/pollutants (SLCFs/SLCPs)*, i.e. black carbon (BC) and ozone (O_3), variability in the southern Himalayas. Over the investigation period (March 2006 – June 2011), BC and O_3 have shown an average value of 208.1 ± 364.1 ng m^{-3} and 48.7 ± 12.6 ppb, respectively. Both BC and O_3 showed a typical yearly cycle with maxima during the pre-monsoon and minima during the monsoon. Significant inter-annual variability has been pointed out for average BC and O_3 values during the pre-monsoon season, especially in April when their highest monthly average values are typically observed at the NCO-P. We showed evidence for a possible influence of open fires occurrence in south Asia on this inter-annual variability.

In order to systematically investigate the role that 5-day old emissions from open fires in south Asia could have in promoting the development of "acute pollution events" at NCO-P, we analysed 5-day back-trajectory ensembles as a function of active open fires detected by the MODIS satellite sensor.

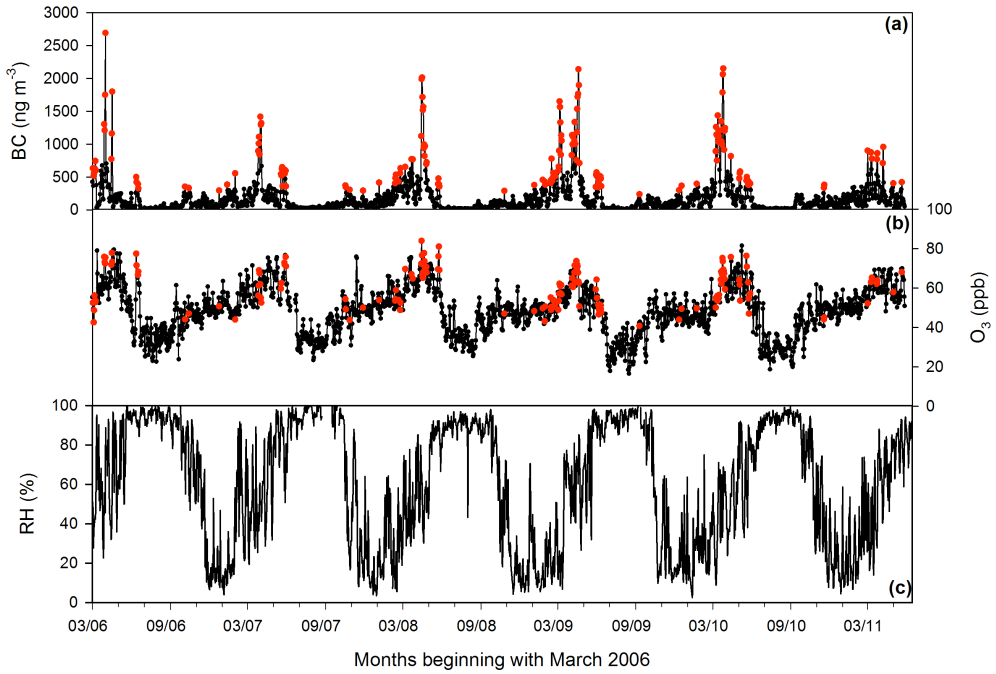

Fig. 2. Daily average values for black carbon (BC, black dotted line, panel a), O_3 (panel b) and relative humidity (RH, panel c) for the period March 2006 – June 2011. Acute pollution events are represented by red dots. RH gives an indication of the wet-dry seasonal transition.

The acute pollution events were selected on a daily basis adopting the methodology reported in Marinoni et al. (*Journal of Environmental Pollution*, 2013), based on a statistically significant exceedance of daily BC averages in respect to the "climatological" values obtained by averaging the yearly time series smoothed by a 21-day running mean. 162 days characterised by very high BC daily levels (here assumed as a tracer for combustion processes) were recognized during the period of interest (see Figure 2).

In order to determine the path of air-masses reaching NCO-P, 5-day longs back-trajectories were calculated by ETHZ (Eidgenössische Technische Hochschule Zürich), using the Lagrangian Analysis Tool (LAGRANTO). Trajectories are calculated every 6 hours (at 00:00, 06:00, 12:00 and 18:00 UTC), starting at the measurement site. The data-base for the

calculation of trajectories is the 6-hourly operational analysis field of the ECMWF. Here, the main variables and the 3-D wind fields are interpolated onto a horizontal 1°x1° grid and calculated with vertical steps of 50 hPa, starting from surface pressure. Subgrid scale processes, such as convection and turbulent diffusion, are not represented by LAGRANTO; to compensate such uncertainties, also 20 additional back-trajectories are calculated, with endpoints shifted by ±1° in latitude/longitude and ±50 hPa in respect to the measurement site location.

In order to identify the measurement periods possibly affected by the transport of open fire emissions, we have coupled the occurrence of fires from MODIS and the 5-day back-trajectory ensembles. Both MODIS/Terra and MODIS/Aqua measurements were considered; in particular, we used the Global Monthly Fire Location Products (MCD14ML). These data contain information about the geographic location, date and some additional features for each fire pixel detected by the MODIS sensors on a monthly basis. A detection confidence is provided as part of the product; for this work, only fires with confidence value ≥ 75% (high-confidence level) are used. First, to retain only fires which were likely to be ascribed to open vegetation burning, we screened the MODIS fire data-base as a function of the land use. For each "acute pollution event", if at least one point of a member of the back-trajectory ensemble overpassed an active fire, the trajectory was flagged as influenced by open fires and the measurements at the NCO-P were tagged to the geographical region where the fire occurred. Basing on this analysis, among 162 polluted days, 90 (56%) showed a direct link with open vegetation fires occurring over central and south Asia. In particular, 78% of the fires have been overpassed over the South Himalayas region (Fig. 3), with the remaining as being distributed over Northern Indo-Gangetic Plain (19%) and Indian Subcontinent (3%).

Assuming that all the observed BC and O_3 can be attributed to the identified fires, we roughly estimated the quantitative contribution that each of the above mentioned regional boxes gave in increasing the BC (O_3) daily concentrations, compared to seasonal averages. The seasonal averages of these differences are indicated as ΔBC and ΔO_3 respectively. During pre-monsoon season, the average ΔBC was maximized (630.1 ± 449.6 ng m^{-3}). Considering all seasons, the

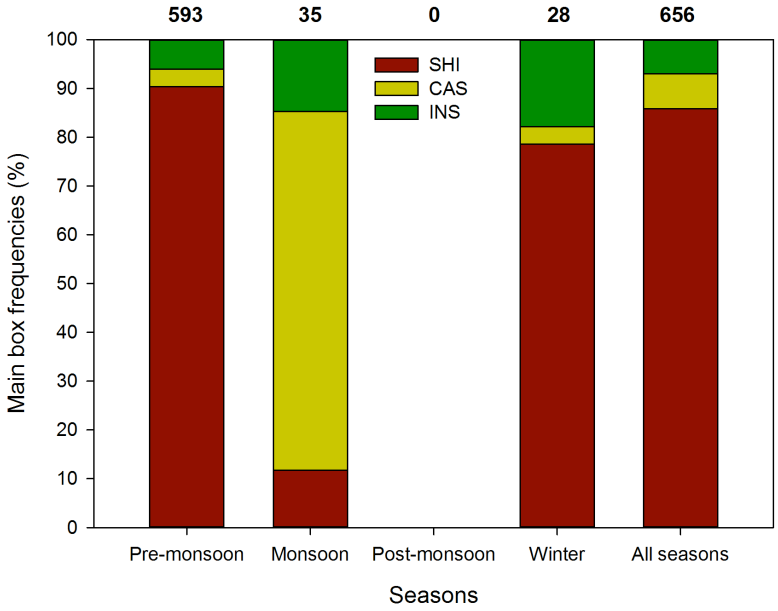

Fig. 3. Main box occurrences (%) for the different seasons during BB acute pollution events. Abbreviations for the box names and box extensions refer to those presented in Table 2. Numbers at the top of each column indicate the total number of occurrences verified during each season.

average ΔBC was 570.5 ± 412.7 ng m^{-3}, with transport from Himalayan foothills playing a dominant role (ΔBC : 388.7 ± 389.1 ng m^{-3}).

Over the whole year, the average ΔO_3 was 8.2 ± 9.5 ppb. Average ΔO_3 increases were far smaller during the pre-monsoon (5.4 ± 6.6 ppb) and Winter (4.1 ± 5.1 ppb) seasons, when the largest ΔO_3 were still tagged to possible fire in the Himalayan foothills (4.5 ± 5.6 and 2.3 ± 3.7 ppb, respectively).
Although a significant fraction (44%) of the pollution events did not show any signal about possible influence of open fire emissions, these preliminary results, together with recent works dealing with the impacts of BC emission on Himalayas cryosphere and south Asia climate, stress the necessity of considering the adoption of mitigation measures to minimize the occurrence of open vegetation fires in the south Himalayas and northern Indo-Gangetic plains.

Research activity: analysis of acute pollution events during the monsoon onset period

NCP-P data series were used to study and characterise the systematic occurrence of elevated levels of SLCFs/SLCPs (BC, aerosol particle and O_3), during the Summer monsoon onset period (May – June). The aim of this investigation (a paper by Adhikary et al. has been submitted to *Environmental Research Letters*) is to contribute to better assess the SLCFs/SLCPs variability in Himalaya as well as their possible relationship with the monsoon circulation. For example, absorbing aerosols (dust and black carbon), may intensify the northern Indian summer monsoon through the so-called "Elevated Heat-Pump" effect (Lau et al., *Geophysical Research Letters*, 2006), while Bollasina et al. (*Journal of Climate*, 2008) argued that excessive aerosol loading during the pre-monsoon season (especially during the month of May) lead to reduced cloud cover and precipitation which in turn heat the land surface that leads to strengthening of the monsoon in June and July. Periods characterised by rain precipitation interruption are typical of the Himalayas before the beginning of the continuous summer monsoon precipitation, during the so-called monsoon onset period (from May to June). As clearly shown by the NCO-P measurements (see Marinoni et al., *Journal of Environmental Pollution* 2013 and Putero et al., *Environmental Pollution* 2013), due to the efficient wet scavenging, the Summer monsoon appears as the season less affected by pollution transport from the Indo-Gangetic Plains. Therefore, the specific aim of this investigation was to verify the possibility that during these periods characterised by "breaks" or decrease in the rain precipitation, significant increases of SLCF/SLCP affected NCO-P and South Himalayas.

We considered three classes of data for this study: in-situ observations, satellites based observations and numerical model products. We analysed in-situ data collected from NCO-P (ozone, BC, PM10) and rain measurements at four Automated Weather Station (AWSs) located along the Khumbu valley: Lukla (2660 m a.s.l., ~31 km from NCO-P), Namche (3560 m a.s.l., ~20 km), Pheriche (4258 m a.s.l., ~7 km) and at the Pyramid laboratory (5050 m a.s.l., 300 m from NCO-P). To provide a robust characterisation of rain occurrence along the Khumbu valley, we considered the daily averaged values of 24-hour cumulated rain at the four stations. The averaging amongst AWS smoothens out biases due to topography as well as the problem associated with spatial representativeness of single point measurements.
To show regional rain precipitation patterns during the monsoon onset period, we used the Tropical Rainfall Measuring Mission (TRMM, see Huffman et al., 2007). Specifically, we used the TRMM_3B42_Daily.007 data for our study. To examine the spatial distribution of absorbing aerosol (dust and pollution), we used the ozone monitoring instrument (OMI) on

board the Aura satellite: the OMI UV aerosol index (AI), data product OMTO3D.003, represents a proxy for the atmospheric aerosol loading.

To study synoptic-scale atmospheric circulation, we used the LAGRANTO back trajectory analysis. To identify the local onset and decay dates of the summer monsoon circulation at the NCO-P, we used the methodology defined by Bonasoni et al. (2010). The monsoon was defined as the period characterised by high relative humidity and the presence of persistent southerly winds during night time at the measurement site. For the considered years, the beginning of the summer monsoon varied from early May to mid-June while monsoon end varied from mid-September to mid-October, thus indicating significant year-to-year variability (Table 1).

During the monsoon onset period, the Himalayas can be affected by changes in air-mass circulation coupled with a break stage of SASM, usually characterised by absence of precipitations. For these onset periods, "pollution" events have been identified at NCO-P since the year 2006 (Table 1). We consider as pollution event, a long lasting period (at least 1 week) characterized by BC concentrations exceeding the typical value for background conditions at NCO-P (100 ng m^{-3}). Our analyses show that the pollution event duration ranged from one week (year 2008) to three weeks (year 2009). For the years 2006, 2008, 2009 and 2011 the pollution events were observed during early period of the summer monsoon season, while for the years 2007 and 2010, they were observed just several days before the calculated monsoon onset dates (Fig. 4).

Year	Averaging Period	Pollutant Concentration								
		O3 (ppb)			BC (ng/m3)			PM10 (µg/m3)		
2006	Monsoon Onset-Decay: 21 May -26 Sep	40	±	11	85	±	115	2.2	±	3.8
	"Peak" event duration: 11 Jun - 21 Jun	63	±	11	287	±	155	9.0	±	6.7
2007	Monsoon Onset-Decay: 6 Jun - 12 Oct	38	±	8	41	±	29	1.1	±	2.8
	"Peak" event duration: 21 May - 04 Jun	66	±	8	421	±	257	12.3	±	9.0
2008	Monsoon Onset-Decay: 10 May - 7 Oct	43	±	12	94	±	115	2.2	±	4.5
	"Peak" event duration: 28 May -03 Jun	69	±	8	329	±	147	9.5	±	5.5
2009	Monsoon Onset-Decay: 21 May - 15 Oct	37	±	12	106	±	152	4.6	±	10.4
	"Peak" event duration: 06 Jun -23 Jun	52	±	5	373	±	184	12.8	±	14.1
2010	Monsoon Onset-Decay: 12 Jun - 24 Sep	34	±	12	48	±	68	0.8	±	1.6
	"Peak" event duration: 9 May - 23 May	67	±	8	287	±	221	15.0	±	8.2
	"Peak" event duration: 29 May - 11 Jun	60	±	10	328	±	168	8.5	±	7.5
2011	Monsoon Onset-Decay: May 27 - 20 Sep	38	±	12	63	±	129	1.3	±	1.9
	"Peak" event duration: 02 Jun - 10 Jun	63	±	7	385	±	242	4.5	±	3.0

Tab. 1. Onset and decay dates of the summer monsoon seasons at NCO-P with the list of peak pollution events from 2006 to 2011, uncertainties for pollutant concentrations are 1 standard deviation from the average values.

Analysis of daily mean precipitation measured along the Khumbu valley during May, June and July for the years 2006-2011 show that these pollution events systematically occurred when very little or almost no precipitation is recorded (Fig. 4). On average, during these events, O_3 showed an increase of at least 40% with respect to the remaining monsoon days, while BC and PM10 increased from 100% to an order of magnitude higher.

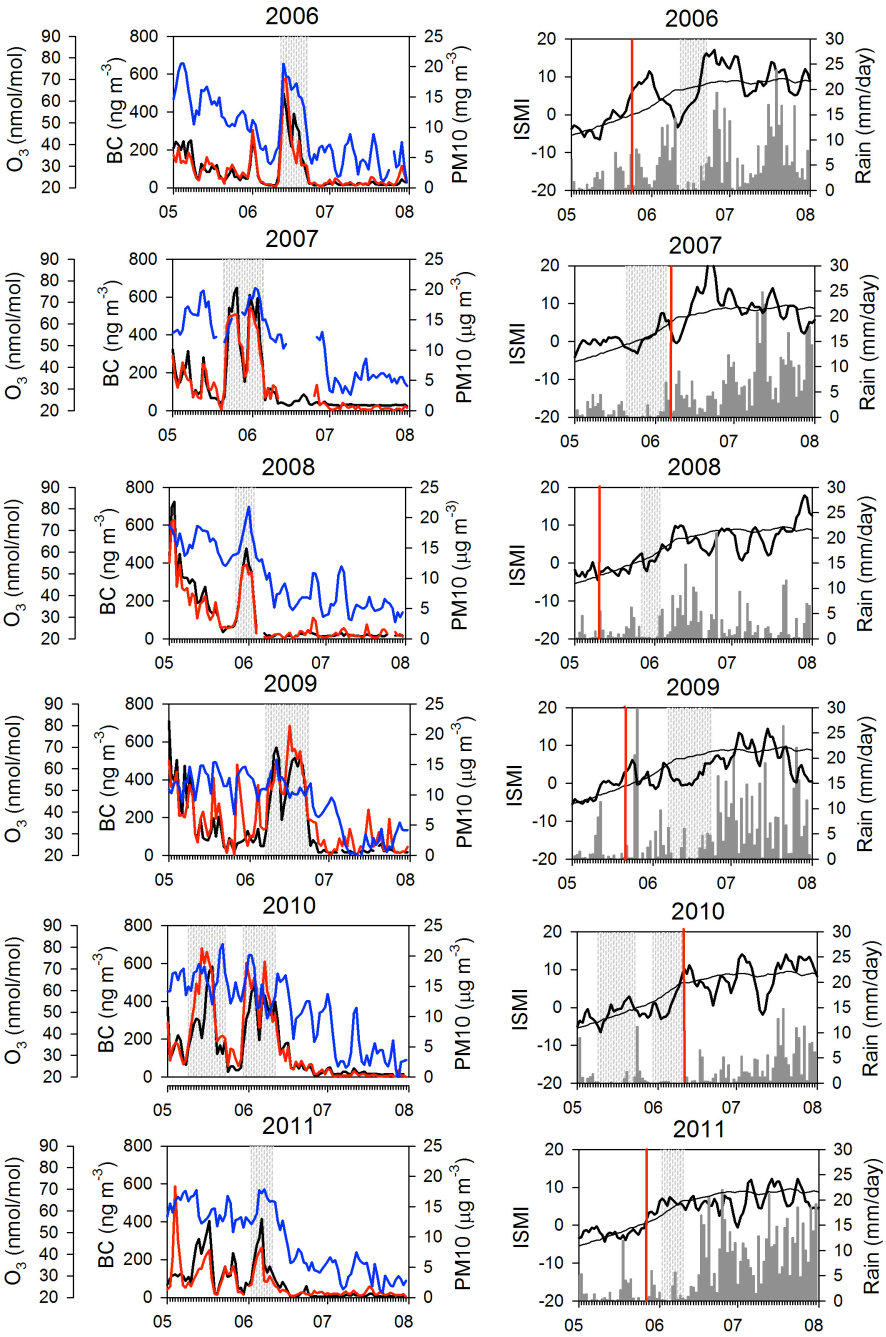

Fig. 4. Left: daily mean values of O_3 (blue), BC (black) and PM10 (red) at the NCO-P for the period 1 May – 31 July for years 2006 – 2011. Right: daily mean precipitation along the Khumbu valley (grey bars), together with actual (thick line) and climatological (thin line) Indian Summer Monsoon Index (ISMI) values. As defined by Wang et al., (2001) this index is calculated using the difference of the 850-hPa zonal winds between a "southern" region of 5°–15° N, 40° –80° E and a "northern" region of 20°–30° N, 70° –90° E. Negative ISMI values indicate a "breaking" or "weak" stage of the SASM, while positive ISMI suggests the occurrence of "active" SASM stage. Shaded areas denoted the event duration, vertical red lines indicate the onset dates of the summer monsoon season at NCO-P based on Bonasoni et al. (2010).

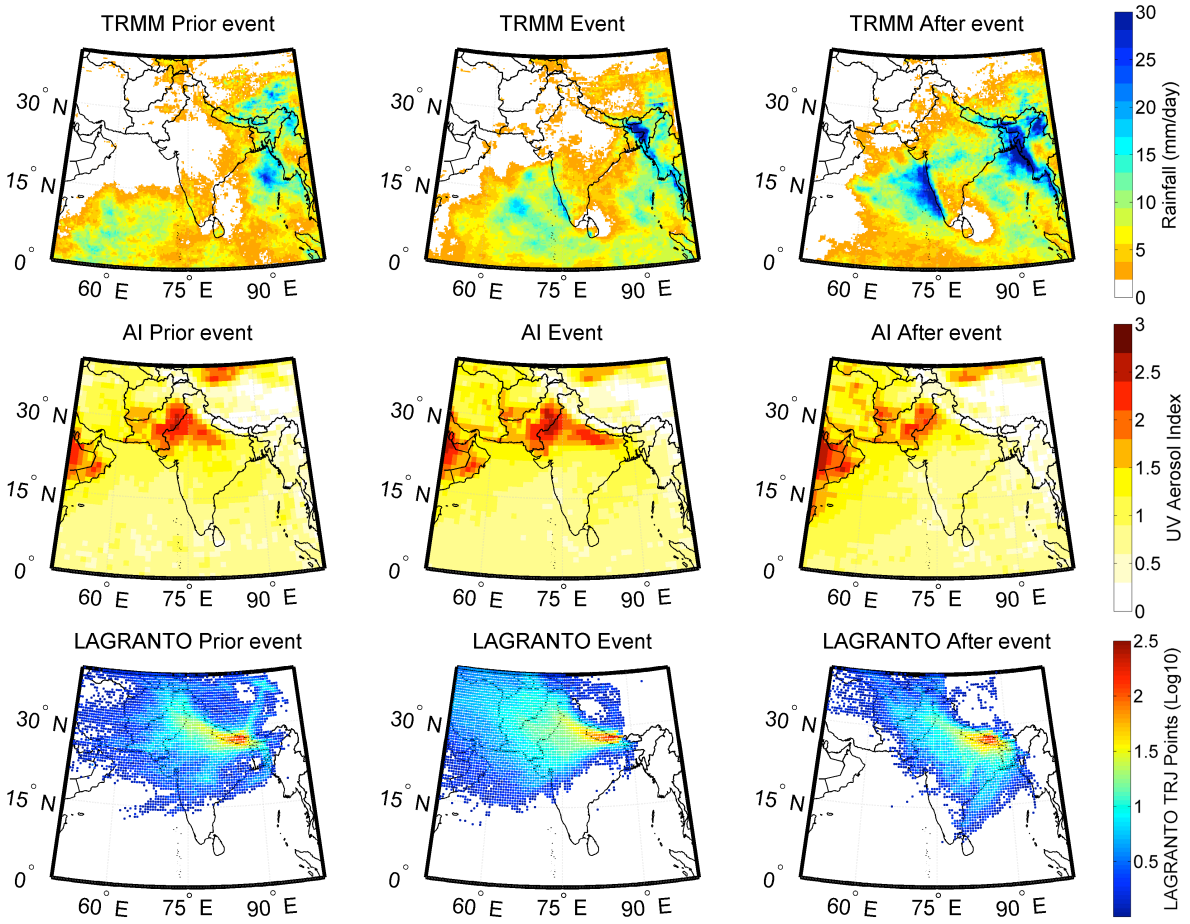

Fig. 5. Distribution of rain precipitation from TRMM, Aerosol Index (AI) from OMI and LAGRANTO model back trajectories for prior, during and after high 'pollution events' at the onset of summer monsoon for the years 2006-2011.

To identify source regions and transport pathways for the air-masses rich in O_3 and aerosol during these pollution events, we analysed the regional distribution of precipitation (TRMM) and absorbing aerosol (OMI AI) as well as air-mass circulation (LAGRANTO back trajectories). In particular, we compared the time period during the pollution events as well as for the 7-day periods preceding and following the events. The choice of 7-day time period before and after was chosen to capture the synoptic variability of rain precipitation and the spatial pattern of the SLCFs/SLCPs. The averaged spatial fields over the years 2006 – 2011 are shown in figure 5. As deduced by TRMM elaboration, before and during the pollution events observed in Himalayas, rain precipitation was almost absent over the entire Ganges Valley, a strong source of anthropogenic pollution. The Indian Thar desert area can also contribute to these events as a source for large amount of airborne mineral dust. As shown by OMI AI, in the days prior and after the events, high aerosol loading is confined to Western India/Pakistan and the Thar desert areas. Otherwise, during the pollution event, high OMI AI values are present across the Ganges valley to east India and the foothills of Himalayas, suggesting transport to the areas adjacent to NCO-P. These evidences suggest that elevated amount of aerosols and O_3 were able to reach the NCO-P during the break periods of monsoon onset, when more zonal atmospheric circulation affected the Himalayan range, as also deduced by LAGRANTO analysis. After the events, when the large-scale monsoon flow was entirely established, the back-trajectories indicated the re-establishment of the usual south/ southeasterly circulation, typical of the Summer monsoon at the NCO-P.

Research activity: analysis of synoptic-scale dust transport in the southern Himalayas

We characterized the synoptic scale mineral dust transport in the Himalayan region basing on five years (March 2006 – February 2011) of continuous observations performed at the NCO-P. Coarse particles number concentrations, $N_{1\text{-}10}$ (1 μm < Dp < 10 μm), considered as a proxy for mineral dust at high altitude remote sites have been used to identify the Dust Transport Days (DTDs). We also characterized the seasonal aerosol size distributions from 0.25 to 10 μm and single scattering albedo (SSA, a key parameter for deriving local estimates of direct aerosol radiative forcing) during DTDs with respect to days without dust transport together with the contribution of different source areas to the mineral dust transported at 5000 m a.s.l. in the Himalayas. The results were submitted to the international journal *Aeolian Research* by Duchi et al.

With the purpose of identifying dust events related to synoptic-scale atmospheric transport, only night-time observations were considered for the analysis (00:00 – 06:00 Nepal Standard Time), when the NCO-P site is well representative of the tropospheric background conditions. The night-time $N_{1\text{-}10}$ time series were analysed (Fig. 6) by using the Kolmogorov-Zurbenko filter, thus highlighting statistically significant increases of the $N_{1\text{-}10}$. These increases were observed for 275 days (corresponding to 22.2% of the investigated period). Thanks to the analysis of LAGRANTO back-trajectories, the predominant source of mineral dust reaching the measurement site was identified in the arid regions of north-western Indian Subcontinent (Thar desert), which accounted for 41.6 % of the trajectories points associated with DTDs. Seasonal analysis also indicated that the winter season was significantly influenced by far western desert regions, such as North Africa and Arabic Peninsula.

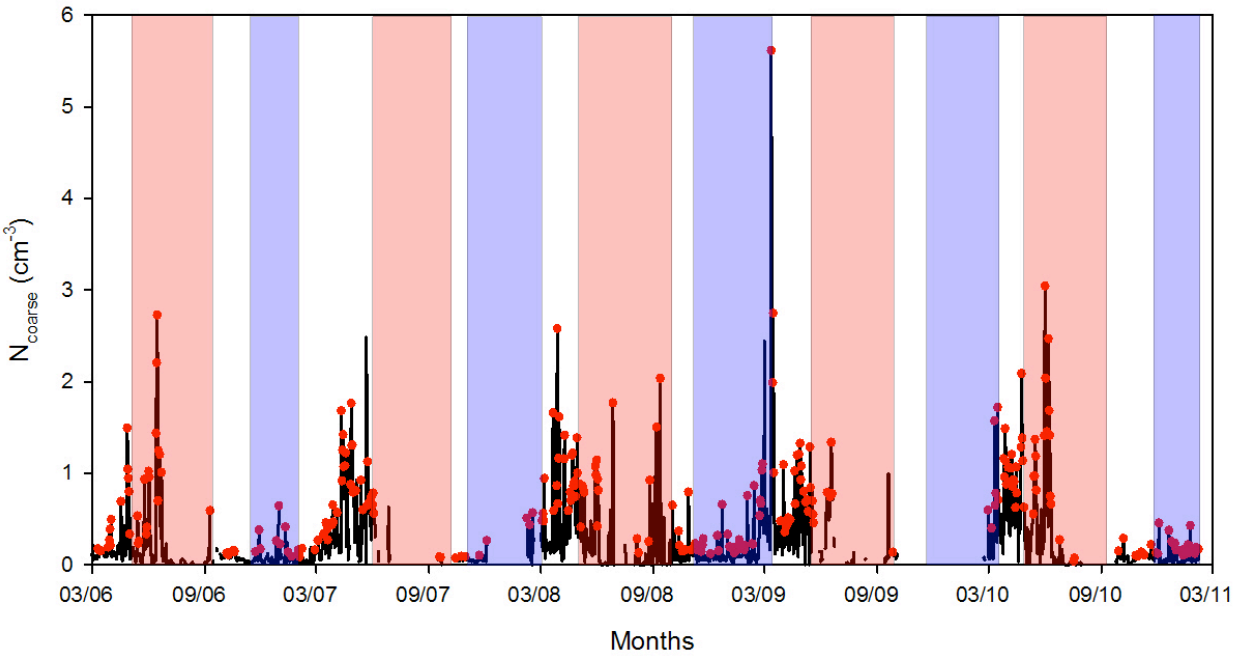

Fig. 6. Night-time (00:00 – 06:00 NST) $N_{1\text{-}10}$ daily average values at NCO-P from March 2006 to March 2011. Red dots indicate DTDs and vertical bars delimit the monsoon (red) and Winter (blue) season.

Over the 5 year period, large enhancements in coarse aerosol number concentration $N_{1\text{-}10}$ (average increase: 0.62 cm-3, +689%) and mass $PM_{1\text{-}10}$ (average increase: 13.5 μg m^{-3}, +435%) were observed during the dust transport events as compared to the average values found in the days without dust (0.09 ± 0.13 cm^{-3} and 3.1 ± 16.8 μg m^{-3}, respectively). In

addition, the single scattering albedo (SSA) also showed higher values, ranging from 0.87 to 0.90, during DTDs with respect to DFDs (0.80 – 0.88).
This reflects the influence of synoptic-scale transport of mineral dust on aerosol optical properties over South Himalayas with possible implication for the aerosol radiative effects over this region. This work indicates that considerable amount of mineral dust is systematically transported towards the Himalayas leading to notable changes in the aerosol particle properties during the observed DTDs. It fills an important gap of knowledge and constitutes a base for future researches on the climate impacts of mineral dust in the Himalayan region. In particular, the study of the interactions between optically active dust and soot particles in the glacier areas of the Himalayas represents a mandatory action for a more accurate estimation of the influence on the radiative balance of the lower atmosphere and on the impact on Himalayan snow cover and glacier dynamics.
The identification of mineral dust source areas has indicated that, on an annual basis, the Indian Subcontinent is the predominant dust source (41.6% of back-trajectory points), with a major contribution from the Thar desert. This is especially true for the monsoon season, while the winter season showed a strong influence from far western desert regions. During the monsoon season significant dust transport can be observed at NCO-P when large-scale shifts in summer monsoon circulation affect the measurement site, leading to a non-negligible contribution from the arid regions of Iran, Afghanistan and Pakistan.

Activities at the Monte Cimone – "O. Vittori" Station (ICO-OV)

According to the "scientific questions" (Deliverable D1.1.1), also thanks to the interaction with the EU Project ACTRIS, two systems for the measurements and the investigation of NO_x and SO_2 variability at the GAW/WMO Global Station Monte Cimone were implemented at the CNR-ISAC laboratories in Bologna. In particular, an enhanced NO_x measurement system was based on the Chemioluminescence detection and was equipped with a photolytic converter. This system was coupled with a calibration device with gas phase tritation and dilution. The installation of the GAW/WMO Global Station at Monte Cimone is foreseen in March 2014. The system is based on a commercial instrument which has been modified in agreement with the feasibility study presented in D1.2.2 with the purpose of reaching the Data Quality Objective indicated by ACTRIS/GAW/WMO for "enhanced" measurement sites (see D1.2.2).

A MoU (Memeorandum of Understanding) was signed between CNR-ISAC and the Earth System Research Laboratory (ESRL) of the National Oceanic and Atmospheric Administration (NOAA) for the provision of calibrated trace gas air standards for CH_4, CO, SF_6, and N_2O. ESRL has become responsible for maintaining the World Meteorological Organization (WMO) mole fraction scales for these compounds with the mission of propagating these scales for data intercomparison. Because of stringent quality controls necessary for the measurement of trace gases, the adoption of these high quality stable reference gas standards are an integral part of the correct implementation of the long-term measurement program. Thus, also thanks to the collaboration with the Urbino University, the adoption of these gas standards will assure the accurate execution of the CH4, CO, N2O and SF6 measurements at the Monte Cimone GAW/WMO Global Station. A pneumatic system to deliver the standard mixtures to the NDIR CO analyser (upgraded during the first year of the Project), was also implemented. During the current reference year, some problems affected the UPS which assure the power continuity to CH4, N2O and SF6 measurements, carried out in collaboration with Urbino University. To cope, CNR-ISAC Bologna technicians upgraded the battery packs of the UPS.
Despite the upgrade of the sampling system carried out during the first year of the project, several technical issues affected the PM1-PM10 sampler (SWAM 5A MONITOR, FAI Instrument S.r.L). During the current year of activity, CNR-ISAC and the manufacturer

technicians operated several interventions: this allowed an increase of the measurement availability during the last part of the year.
In December 2013, a further MoU was signed with the Barcelona Supercomputer Center (BSC) for the near-real-time (NRT) provision of aerosol data (PM10, PM1, accumulation and coarse particle number concentrations) to the WMO Sand and Dust Storm Warning Advisory and Assessment System. To this aim, a system for automatic pre-validation and delivery of hourly data has been implemented at CNR-ISAC Bologna and, starting from January 2014, hourly average value of coarse and accumulation aerosol particle number will be send to BSC (see http://sds-was.aemet.es/news/in-situ-measurements-from-mt.-cimone).
Starting from 2013, a NRT data delivery service was made operative at the ICO-OV to provide hourly CO mixing ratio to the MACC-2 UE-Project. Data are automatically pre-elaborated and pre-validated and delivered to ECMWF servers for the NRT evaluation of the Integrated Forecast System for the atmospheric composition variability (see http://gmes-atmosphere.eu/d/services/gac/verif/grg/gaw/gaw_station_ts!All!Mt.%20Cimone!Carbon%20monoxide!macc!od!enfo!gaw_station_ts!201306!/).
With the purpose of prosecuting the implementation of a continuous monitoring programme for aerosol LIDAR observations, a specific heated window was built on the roof of the station which has been equipped with suitable devices for hosting a LIDAR system. Moreover, a permanent permit to operate (NOTAM) from the National Aviation Authorities was achieved. This will allow to permanently install at the ICO-OV the LIDAR developed by CNR-ISAC Bologna and tested at ICO-OV during the first year of the project (see WP1.2, first year). Unfortunately, due to a major problem to the laser source, this system was out of order for the whole year 2103 but the final installation is foreseen in Spring 2014.
A feasibility study was carried out to implement aerosol optical depth (AOD) measurements at the ICO-OV with the purpose of fulfill to the GAW/WMO recommendation concerning the execution of high-quality AOD measurements at the Global Stations. In particular, thanks to the collaboration with PMOD/WRC (Physics Meteorological Observatory - World Radiation Center in Davos, Switzerland) a PFR (Precision-Filter-Radiometer) sunphotometer will be installed at Monte Cimone during year 2014.
With the aim to fulfill in the recommendations defined during the first year of the Project (see Deliverables D1.1.1 and D1.2.1), several upgrade activities (presented by the Deliverable D1.2.5) were carried out concerning the aerosol observation programmes. In particular, the system (a Differential Mobility Particle Sizer) for the investigation of the aerosol size distribution of particles with diameters from 10 nm to 800 nm has been completely renewed according to GAW/ACTRIS recommendations. Moreover, the aerosol scattering coefficient measurement programme (active since 2007) was upgraded by implementing a three-wavelength (at 450, 525 and 700 nm) integrating nephelometer, which will be installed at Monte Cimone in February 2014. Finally, the measurement of the aerosol size distribution from 500 nm to 20 μm based on time of flight was set up in July 2013.
During the reference period, analyses of historical data (April – May 2010) were performed to investigate the impact of the in-situ physical and chemical characterization of the Eyjafjallajökull aerosol plume in the free troposphere over Italy (see Sandrini et al., ACP, 2014). Moreover, the following researches were carried out by analyzing data from Monte Cimone.

Research activity: Analysis of long-term surface ozone trend at the Italian Climate Observatory "O. Vittori" at Monte Cimone

The Mediterranean basin represents a hot-spot area in terms of short-term O_3 distribution and anthropogenic contributions to it. Like in other regions of the world, surface O_3 have doubled in the Mediterranean basin compared to pre-industrial ages due to the combination of regional precursor emission growth and, possibly, inputs related with intercontinental transport. Because of the typical anticyclonic conditions of the Mediterranean basin, intensive O_3 photochemical production events frequently occur in this region during the warm period.

While several studies have been performed for evaluating long-term surface O_3 variability and trends at remote and rural locations of continental Europe, no specific efforts have been conducted to evaluate the long-term O_3 trends in the Mediterranean basin. For these reasons, we analysed the long-term time series of surface O_3 observations at CMN from 1991 to 2011. The study aims at providing information on long-term surface O_3 variability at this high mountain site that, as being located South of the Alps in the Apennines, can be considered representative (especially during the cold months) for the lower troposphere conditions of the Mediterranean basin/southern Europe (MB/SE). Due to its proximity to the Po basin, a hot-spot region for air pollution, the CMN observations can provide useful hints to investigate the influence of anthropogenic pollution mixing along the lower troposphere.
At CMN, the first surface O_3 measurements were carried out in the period 1991 – 1993 by CNR-ISAC at the Air Force Meteorological Observatory, which is located about 50 m. higher than the current location of the measurement site (the ICO-OV Observatory). We cannot completely rule out the existence of artificial bias between the 1991 – 1993 and the 1996 – 2011 data sets, thus we decided to analyse the long-term trends of surface O_3 in a "segmented" way: linear regressions of monthly mean anomalies were calculated over two reference periods:

(a) over the whole measurement period, also encompassing the earlier measurements (1991-1993) performed at the Air Force Observatory, i.e. 1991 – 2011;
(b) over the period for which measurements were continuously carried out at the ICO-OV, i.e. 1996 – 2011.

With the aim of evaluating the statistical significance of the calculated trend, the 95% confidence level of the growth rates has been calculated as ± 2σ.
As reported in Figure 6, positive trends characterised monthly O_3 mixing ratios at CMN during the entire period, with averages slopes (0.21 ± 0.10 nmol/mol yr^{-1}). As clearly shown by the time series of O_3 monthly anomalies (Fig. 7), the 1991-2011 positive trends were strongly influenced by the presence of negative values occurring during the years 1991-1993. When the period 1996-2011 is considered, very small tendencies (not different from zero) have been calculated. As a further investigation, we analysed the seasonal long-term variability by interpolating the annual mean O_3 averages with a polynomial quadratic fit for the period 1991 – 2011 and 1996 – 2011 (Fig. 8). For the polynomial fit, the slope K1 provides the interpolated, seasonally averaged rate of increase of O_3 in year 2000 and 2003 which have been defined as "reference years" for a direct comparison with the results presented by Parrish et al. (2013) for other baseline stations in the world. As specified in this previous work, this rate of increase changes with time rather than representing the average yearly increase as is the case of a linear fit. The "acceleration" (expressed as nmol/mol yr^{-1}), represents an indication of the rate of change in the O_3 growth rate and equals the average rate of increase of the slope over the period of the data record. The fitting is independent of the choice of reference year.
Concerning the quadratic regression, for the period 1991 – 2011, statistically significant negative accelerations are found at CMN in all season except for autumn, indicating a slowing

of the O_3 increase rate. Considering the years 1996 – 2011, a statistically (even if marginally) significant (negative) acceleration is found only for the summer season.

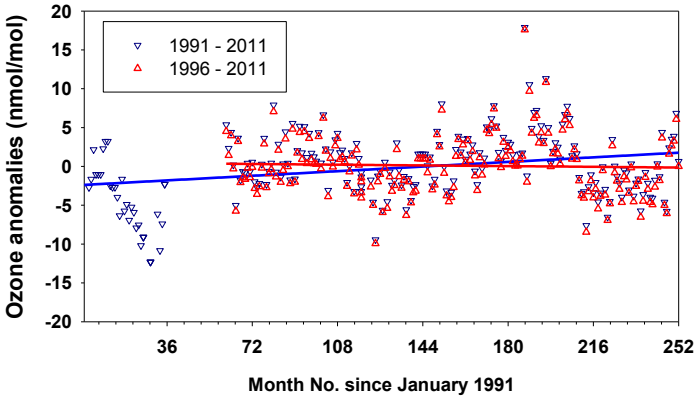

Fig. 7. Monthly O_3 anomalies and linear trend fitting (continuous lines) for the period 1991 – 2011 (blue) and 1996 – 2011 (red), based on the "all data" selection.

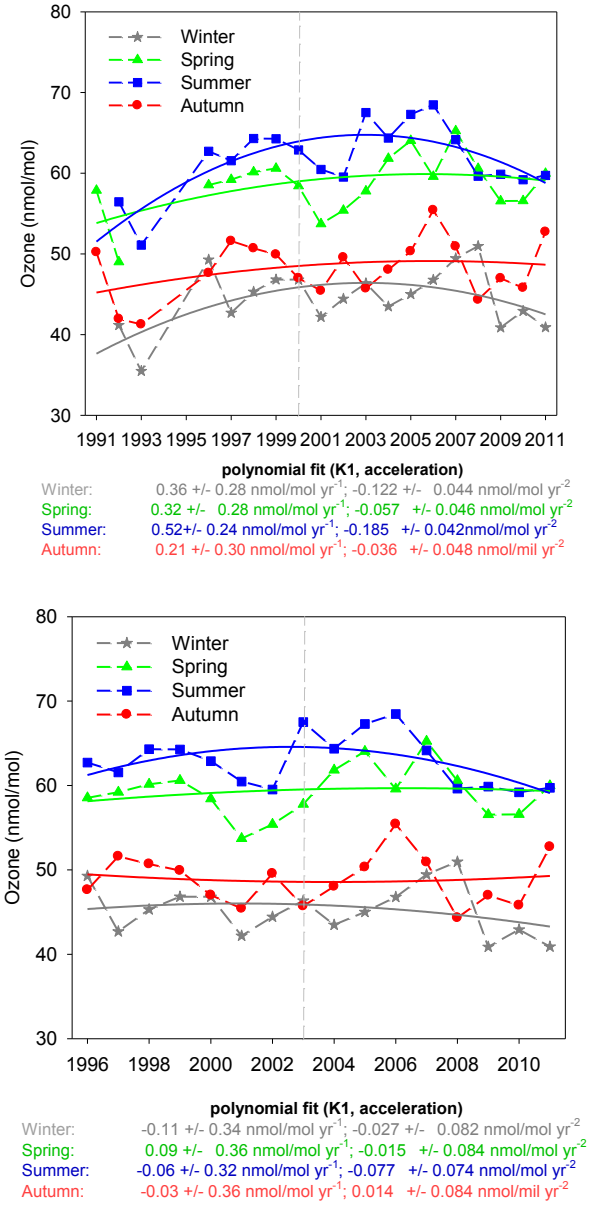

Fig. 8. Seasonal O_3 averages measured at CMN for 1991 – 2011 (upper plate) and 1996 – 2011 (bottom plate). The solid lines indicate quadratic regressions for the entire data sets. The annotations in each figure give the derived parameters of those regressions, along with their confidence limits (±2σ).

Research activity: seasonal report on atmospheric composition at the Italian Climate Observatory "O. Vittori" at Monte Cimone

With the aim of providing updated and accurate information about the "state of the atmosphere", as seen by the observations carried out at the ICO-OV, the behaviour of atmospheric parameters (trace gases, aerosol, meteorological parameters) was investigated for the Summer 2013. In particular, for each atmospheric parameter, we provided basic statistical information (minimum, maximum and average values) together with a comparison with the climatological reference values for Mt. Cimone. For each observed parameter, we specifically presents:

- the time series of the daily mean values (calculated basing on 30-minute aggregated values, if the daily data coverage of 75% has been achieved);
- a table reporting the basic statistical parameters (on a 30-minute basis);
- a comparison with the seasonal historical mean values: for each year, the summer mean values are calculated by averaging data from June 1st to August 31st.

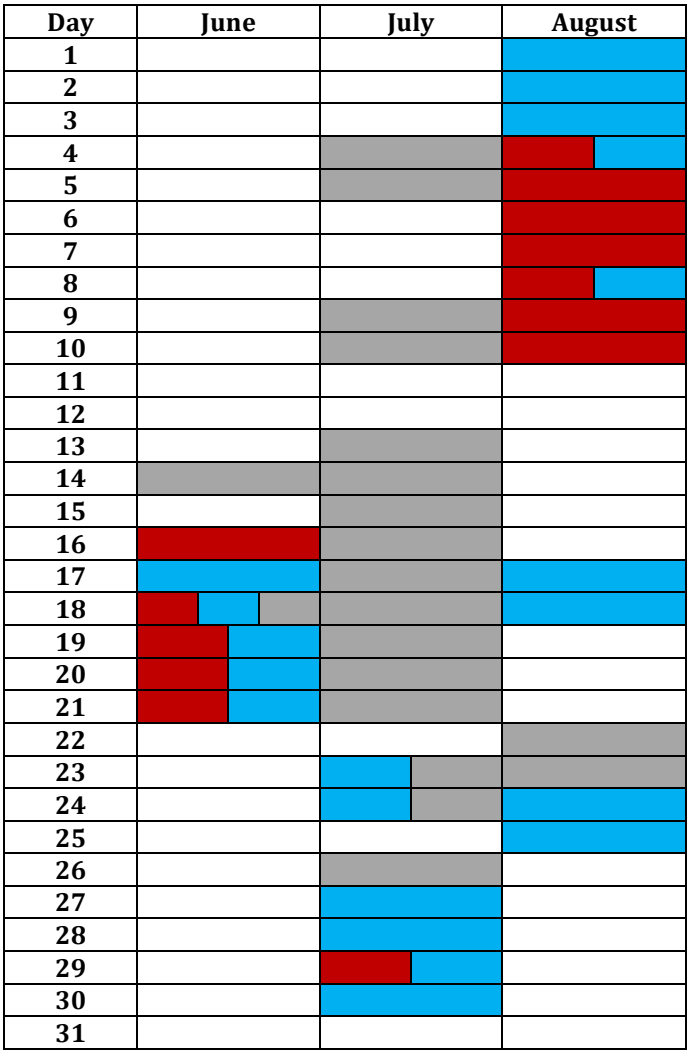

LEGEND

Mineral dust Stratospheric intrusions Pollution transport

Tab. 2. Overview of "special events" which have been detected at the ICO-OV during Summer 2013. It must be noted that the event selection methodologies are executed on 30-minute basis, thus, for the same day, different classes of special events can be observed. Extracted from http://www.isac.cnr.it/cimone/reports.

Moreover, a list of special events (i.e. pollution transport, mineral dust transport, transport of air-masses from the stratosphere) which occurred during Summer 2013 was also presented together with a description of the adopted selection methodologies (Table 2). Based on these analyses, Summer 2013 did not present high average levels of short-lived climate forcers (SLCF): a value similar to the climatological mean was observed for surface ozone while for black carbon, it was lower. Also coarse particles were comparable with the climatological value. Only for fine particles we reported higher average value in respect with previous summer seasons.
During Summer 2013, 20.4% of the summer days have been affected for a significant fraction of time by transport of polluted air-masses. On a monthly basis, June and August 2013 appeared less polluted than July, which instead accounted for 79% of the polluted days, also showing the highest values of ozone, carbon monoxide, black carbon and fine particles. 13 days were affected by mineral dust transport, with a major event which occurred from August 4^{th} to 10^{th}, when very high air temperatures (19.1 °C) were also observed. Air-mass transport from the stratosphere occurred for 21.7% of the period and have been almost equally distributed among the three months. These information have been summarized in a seasonal report that will be published quarterly on-line (ISSN: 2283-9631) at
http://www.isac.cnr.it/cimone/reports.

Data availability

Summary of data transmitted to the NextData archives for the "**O. Vittori" GAW/WMO Global Station at Monte Cimone** (part of the data-series were obtained in the framework of SHARE and other Research Projects):

Meteorology: Start date: January 1996; End date: Ongoing; Instrument: IRDAM WS7000: Vaisala WS425; Validated data availability: from January 1996 to December 2012; Data Format: WDCGG Version 1.0; Data provider: ISAC-BO.

O_3 mixing ratio: Start date: January 1996; End date: Ongoing; Instrument: Daisibi 1108 W/GEN; Validated data availability: from January 1996 to December 2012; Data Format: WDCGG Version 1.0; Data provider: ISAC-BO.

CO mixing ratio (NDIR): Start date: June 2012; End date: Ongoing; Instrument: Thermo Electron Tei 48C; Validated data availability: from August 2010 to December 2012; Data Format: WDCGG Version 1.0; Data provider: ISAC-BO.

CO mixing ratio (GC-RGD and GC-FID): Start date: February 2007; End date: Ongoing; Instrument: customized GC-RGD (RGD2-Trace Analytical) and GC-FID (Agilent 6890N); Validated data availability: from February 2007 to December 2011; Data Format: WDCGG Version 1.0; Data provider: Urbino University/ISAC-BO.

CH4 mixing ratio (GC-FID): Start date: January 2008; End date: Ongoing; Instrument: Agilent GC6890; Validated data availability: from January 2008 to December 2011; Data Format: WDCGG Version 1.0; Data provider: Urbino University/ ISAC-BO.

N2O, SF6 mixing ratio (GC-ECD): Start date: November 2008; End date: Ongoing; Instrument: Agilent GC6890; Validated data availability: from January 2008 to November 2012; Data Format: WDCGG Version 1.0; Data provider: Urbino University/ ISAC-BO.

NO and NO2 mixing ratio (Chemioluminescence with Mo converter): Start date: August 2010; End date: Ongoing; Instrument: Thermo Tei 42; Validated data availability: from August 2010 to December 2012; Data Format: WDCGG Version 1.0; Data provider: ISAC-BO.

Solar radiation (at λ 350 – 1100 nm and λ 280 – 315 nm): Start date: January 2012; End date: Ongoing; Instrument: silicon cell pyranometer (Skye SKS110) and a silicon photodiode (Skye SKU 430); Validated data availability: from January2012 to December 2012; Data Format: WDCGG Version 1.0; Data provider: ISAC-BO.

Size distribution of atmospheric aerosol in the 10 – 500 nm range: Start date: November 2005; End date: Ongoing; Instrument: customized Differential Mobility Particle Sizer (DMPS); Validated data availability: from November 2005 to December 2012; Data Format: NASA-AMES; Data provider: ISAC-BO.

Size distribution of atmospheric aerosol in the 300 – 20000 nm range: Start date: August 2002; End date: Ongoing; Instrument: Grimm 1.108 Optical Particle Counter; Validated data availability: from August 2002 to December 2012; Data Format: NASA-AMES; Data provider: ISAC-BO.

Aerosol scattering coefficient at 525 nm: Start date: May 2007; End date: Ongoing; Instrument: M9003 integrating nephelometer (ECOTECH); Validated data availability: from May 2007 to December 2012; Data Format: NASA-AMES; Data provider: ISAC-BO.

Aerosol number concentration: Start date: March 2008; End date: Ongoing; Instrument: condensation particle counter (TSI model 3772); Validated data availability: from March 2008 to December 2012; Data Format: NASA-AMES; Data provider: ISAC-BO.

Aerosol absorption coefficient at 635 nm: Start date: May 2005; End date: Ongoing; Instrument: MAAP, Model 5012 – Thermo Electron Corporation; Validated data availability: from May 2005 to December 2012; Data Format: NASA-AMES; Data provider: ISAC-BO.

Aerosol chemistry: Start date: February 2006; End date: Ongoing; Instrument: PM1-PM0 sampler (off-line analysis at the ISAC-BO laboratories in Italy); Validated data availability: from February 2006 to December 2012; Data Format: NASA-AMES.

Summary of data transmitted to the NextData general portal for for the **Nepal Climate Observatory - Pyramid** GAW/WMO Global Station (these data-series have been obtained in the framework of the SHARE and UNEP-ABC Projects):

Aerosol absorption coefficient at 635 nm: Start date: March 2006; End date: Ongoing; Instrument: MAAP, Model 5012 – Thermo Electron Corporation; Validated data availability: from March 2006 to December 2012; Data Format: NASA-AMES.

Ozone mixing ratio: Start date: March 2006; End date: Ongoing; Instrument: Thermo Electron Tei49C; Validated data availability: from March 2006 to December 2012; Data Format: WDCGG Version 1.0.

Greenhouse Gases mixing ratio (halogenated): Start date: March 2006; End date: Ongoing; Instrument: flask sampling (off-line analysis at the Mt. Cimone GAW/WMO station); Validated data availability: from March 2006 to December 2012; Data Format: WDCGG Version 1.0.

Size distribution of atmospheric aerosol in the 10 – 800 nm range: Start date: March 2006; End date: Ongoing; Instrument: customized Scanning Mobility Particle Sizer (SMPS); Validated data availability: from March 2006 to December 2006; Data Format: ABC-ADAC; Data provider: ISAC-BO/CNRS-LGGE

Size distribution of atmospheric aerosol in the 300 – 32000 nm range: Start date: March 2006; End date: Ongoing; Instrument: Grimm 190 Optical Particle Counter; Validated data availability: from March 2006 to December 2011; Data Format: ABC-ADAC; Data provider: ISAC-BO

Aerosol scattering coefficient at 450, 525 and 700 nm: Start date: March 2006; End date: Ongoing; Instrument: integrating nephelometer (TSI); Validated data availability: from March 2006 to December 2006; Data Format: ABC-ADAC; Data provider: ISAC-BO (CNRS-LGGE).

Wet precipitation chemistry: Start date: June 2012; End date: Ongoing; Instrument: rain gauge (off-line analysis at the IRSA-CNR laboratories in Italy); Validated data availability: from June 2012 to March 2013; Data Format: WDCP.

Aerosol chemistry: Start date: February 2006; End date: Ongoing; Instrument: PM1-PM0 sampler (off-line analysis at the ISAC-BO laboratories in Italy); Validated data availability: from February 2006 to December 2006; Data Format: ABC-ADAC.

Solar irradiance (at λ: 200 - 3600 nm): Start date: March 2006; End date: Ongoing; Instrument: Pyranometer CMP21 Kipp&Zonen; Validated data availability: from January to December 2012; Data Format: GAW/WMO.

IR irradiance (at λ 3.5 to 50 \302\265m): Start date: March 2006; End date: Ongoing; Instrument: Precision Infrared Radiometer-PIR Eppley; Validated data availability: from January to December 2012; Data Format: GAW/WMO.

Meteorology (temperature, relative humidity, atmospheric pressure, wind direction and intensity): Start date: March 2006; End date: Ongoing; Instrument: Vaisala WXT520; Validated data availability: from March 2006 to December 2012; Data Format: WDCGG Version 1.0.

Summary of data transmitted to the Nextdata general portal for **the GAW/WMO Regional Station at Plateu Rosa**

O_3 mixing ratio: Start date: January 2007; End date: Ongoing; Instrument: Environmental 41M up to June 2011 and Thermo 49i from July 2011; Validated data availability: from January 2007 to December 2012; Data Format: WDCGG Version 1.0; Data provider: RSE SpA

CO_2 mixing ratio (NDIR): Start date: April 1993; End date: Ongoing; Instrument: Since 2003 Ultramat 5E NDIR Siemens, since 2008, Ultramat 6E NDIR Siemens; Validated data availability: from January 2000 to December 2012; Data Format: WDCGG Version 1.0; Data provider: RSE Spa

CH_4 mixing ratio (GC-FID): Start date: May 1991; End date: Ongoing; Instrument: Nira VENUS 301 (since November 2007); Validated data availability: from January 2005 to December 2012; Data Format: WDCGG Version 1.0; Data provider: RSE SpA

ANNEX 1- TEMPORAL AVAILABILITYOF THE MEASUREMENTS IN THE FRAMEWORK OF GAW/WMO FOR THE TWO GLOBAL STATIONS "O. VITTORI" – MONTE CIMONE AND NEPAL CLIMATE OBSERVATORY – PYRAMID

O. VITTORI" – MONTE CIMONE (GAW-ID: CMN)

Measurements	JFM	AMJ	JAS	OND
Meteorological data				
Carbon monoxide (NDIR)				
Carbon monoxide (GC-FID)				
Surface ozone				
Methane				
Nitrous Oxide				
Sulfur Hexafluoride				
Nitrogen oxides				
Total particle number concentration				
Equivalent black carbon concentration/aerosol absorption coefficient 635 nm				
Aerosol scattering coefficient at 525 nm				
Size distribution of atmospheric aerosol in the 10 – 500 nm range				
Aerosol chemistry				

NEPAL CLIMATE OBSERVATORY – PYRAMID (GAW ID: PYR)

Measurements	JFM	AMJ	JAS	OND
Surface ozone				
Air temperature				
Atmospheric pressare				
Relative humidity				
Wind direction				
Wind Intensity				
Rain precipitation				
Equivalent black carbon concentration/aerosol absorption coefficient 635 nm				
Size distribution of atmospheric aerosol in the 0.25 – 32 μm range				
Size distribution of atmospheric aerosol in the 10 – 800 nm range				
Aerosol scattering coefficient at 450-525-700 nm				
Aerosol chemistry				
Wet/snow precipitation chemistry				

LEGEND:
- More than 75 % of data available
- Data availability between 50 and 75 %
- Less than 50 % of data available
- Instrument not installed

ANNEX 2- PUBLIC DATA AVAILABILITY FOR THE GLOBAL STATION "O. VITTORI" – MONTE CIMONE

"O. VITTORI" – MONTE CIMONE (GAW-ID: CMN)

Measurements	GAW-WDCGG	GAW-WDCA
Carbon monoxide (GC-RGD)	2007-02-01 - 2010-03-01	
Carbon monoxide (GC-FID)	2008-01-01 - 2011-12-31	
Carbon monoxide (NDIR)	2012-06-12 - 2012-12-31	
Surface ozone	1996 - 2012	
Methane	2008-07-01 - 2011-12-31	
Nitrous Oxide	2008-01-01 - 2011-12-31	
Sulfur Hexafluoride	2008-01-01 - 2011-12-31	
Total particle number concentration		2008-01-01 2012-12-31
Equivalent black carbon concentration/aerosol absorption coefficient 635 nm		2007-01-01 2012-12-31
Aerosol scattering coefficient at 525 nm		2007-01-01 2012-12-31
Size distribution of atmospheric aerosol in the 10 – 500 nm range		2006-01-01 2012-12-31
Aerosol chemistry		2009-02-24 2012-12-31

LEGEND:

♦**GAW-WDCGG**: Global Atmosphere Watch - World Data Center for Greenhouse Gases (http://ds.data.jma.go.jp/gmd/wdcgg/wdcgg.html)

♦**GAW-WDCA**: Global Atmosphere Watch - World Data Center for Aerosol (http://ebas.nilu.no/Default.aspx)

ANNEX 3- PUBLIC DATA AVAILABILITYOF FOR THE GLOBAL STATION NEPAL CLIMATE OBSERVATORY – PYRAMID

NEPAL CLIMATE OBSERVATORY – PYRAMID (GAW ID: PYR)

Measurements	GAW-WDCGG	GAW-WDCA	GAW-WDPC	ABC-DISC	ABC-ADAC	AERONET
Aerosol number concentration and size distribution in the range 250 nm to 32 µm				2006-3-1 2006-12-31	2006-3-1 2011-12-31	
Aerosol number concentration and size distribution in the range 10 nm to 650 µm				2006-3-1 2006-12-31	2006-3-1 2006-12-31	
Total and back scattering coefficient at 450, 550 and 700 nm				2006-3-1 2006-12-31	2006-3-1 2006-12-31	
Aerosol optical depth				2006-3-1 2007-2-28	2006-3-1 2007-2-28	2006-3-27 2012-12-31
Surface ozone	2006-3-1 2012-12-31			2006-3-1 2006-12-31	2006-3-1 2012-12-31	
Chemical mass closure of aerosol				2006-2-20 2006-12-6	2006-2-20 2006-12-6	
Wet/Snow precipitation chemistry			2012-07-04 2012-09-10			
Greenhouse Gases mixing ratio (halogenated)	2006-02-19 2012-12-04			2006-3-1 2007-2-28	2006-02-19 2012-12-04	
Meteorology	2006-3-1 2012-12-31			2006-3-1 2006-12-31	2006-3-1 2012-12-31	
Equivalent black carbon concentration/aerosol absorption coefficient 635 nm		2006-3-1 2012-12-31		2006-3-1 2006-12-31	2006-3-1 2012-12-31	

LEGEND:

♦**GAW-WDCGG**: Global Atmosphere Watch - World Data Center for Greenhouse Gases (http://ds.data.jma.go.jp/gmd/wdcgg/wdcgg.html)

♦**GAW-WDCA**: Global Atmosphere Watch - World Data Center for Aerosol (http://ebas.nilu.no/Default.aspx)

♦**ABC-DISC:** Atmospheric Brown Clouds Data and Information Service Center (http://www.rrcap.ait.asia/abc/data/abc/)

♦**ABC-ADAC:** Atmospheric Brown Clouds Asia Data Analysis Center (http://abc-data.snu.ac.kr/; autentication required)

♦**AERONET**: Aerosol Robotic Network (http://aeronet.gsfc.nasa.gov/cgi-bin/webtool_opera_v2_new)